Neurobiology of Pain 10 (2021) 100071

Contents lists available at ScienceDirect

Neurobiology of Pain

journal homepage: www.sciencedirect.com/journal/neurobiology-of-pain

Original Research

# Annexin A2 traps mu-opioid receptors in recycling endosomes upon remifentanil-induced internalization

Idy H.T. Ho [a,b], Lhotse H.L. Ng [a,b], Xiaojie Cheng [a], Tony Gin [a,b], Chee Sam Chan [a], Wuping Sun [e], Lizu Xiao [e], Lin Zhang [a,b], Matthew T.V. Chan [a,b], William K.K. Wu [a,b,c,d,*], Xiaodong Liu [a,b,*]

[a] Department of Anaesthesia and Intensive Care, The Chinese University of Hong Kong, Prince of Wales Hospital, Hong Kong Special Administrative Region, China
[b] Peter Hung Pain Research Institute, Li Ka Shing Institute of Health Sciences, The Chinese University of Hong Kong, Hong Kong Special Administrative Region, China
[c] Institute of Digestive Disease, Li Ka Shing Institute of Health Sciences, Chinese University of Hong Kong, Hong Kong Special Administrative Region, China
[d] State Key Laboratory of Digestive Disease, Chinese University of Hong Kong, Hong Kong Special Administrative Region, China
[e] Department of Pain Medicine and Shenzhen Municipal Key Laboratory for Pain Medicine, Shenzhen Nanshan People's Hospital and the 6th Affiliated Hospital of Shenzhen University Health Science Center, National Key Clinical Pain Medicine of China, Shenzhen 518060, China

ARTICLE INFO

*Keywords:*
ANXA2
MOR1
Remifentanil
MOR1 internalization

## Introduction

Remifentanil is a synthetic opioid that is commonly used during anaesthesia owing to its rapid onset, ultra-short duration of action and quick recovery (Thompson and Rowbotham, 1996). Intraoperative use of remifentanil was, however, associated with paradoxically increased pain hypersensitivity, commonly known as opioid-induced hyperalgesia, and significant additional amount of opioid was required for postoperative analgesia, suggesting acute analgesic opioid tolerance (Komatsu et al., 2007; Guignard et al., 2000; Crawford et al., 2006; Suhitharan et al., 2018; Wu et al., 2019; de Hoogd et al., 2018; Sanfilippo et al., 2016; Grape et al., 2019; Fletcher and Martinez, 2014; Motamed et al., 2017). Development of acute opioid-induced receptor tolerance remains a major focus in understanding the underlying mechanism of this observation (Guignard et al., 2000; Vinik and Kissin, 1998).

Mu-opioid receptors (MOR) are G-protein-coupled receptors (GPCRs) expressed in dorsal root ganglion (DRG), spinal cord dorsal horn, and multiple brain regions involved in nociceptive information processing (Wang et al., 2018). Delineation of the life cycle of MOR1, including biosynthesis, subcellular distribution, recycling and degradation, is the grounds for understanding MOR1 ligand-initiating phenotypes. Opioid administration may cause surface functional MOR down-regulation by inducing phosphorylation and endocytosis, which contribute to the receptor desensitization or short-term tolerance (Williams et al., 2013). In neuronal cell bodies, morphine tolerance is associated with rapid MOR sensitization, and impaired subsequent recovery or recycling following endocytosis (Williams et al., 2013). Emerging evidence suggests that, in parallel to other GPCRs, protein–protein interactions regulate the structural and functional organization of the MOR signaling complexes. More than 20 MOR-interacting proteins have been identified to non-canonically modulate MOR cell signaling, trafficking, and subcellular localization, and may therefore affect opioid-induced pain perception, analgesic tolerance and dependence (Georgoussi et al., 2012; Milligan, 2005; Petko et al., 2013). For instance, β-arrestin as an MOR-interacting protein is crucial for the desensitization, internalization, degradation and recycling of MOR in the canonical MOR signalling pathway (Marie et al., 2006). Morphine physically binds with and induces redistribution of Wntless from cytoplasmic to membrane compartments in the rat locus coeruleus, contributing to MOR membrane localization (Jaremko et al., 2014). MOR also interacts with spinophilin, leading to MOR signaling modulation and endocytosis (Charlton et al., 2008).

Given multiple MOR-interacting proteins could affect the signalling properties of MOR and mediate its function, we hypothesised that

* Corresponding authors at: Department of Anaesthesia and Intensive Care, The Chinese University of Hong Kong, Hong Kong Special Administrative Region, China.
*E-mail addresses:* wukakei@cuhk.edu.hk (W.K.K. Wu), xdliu@cuhk.edu.hk (X. Liu).

https://doi.org/10.1016/j.ynpai.2021.100071
Received 29 March 2021; Received in revised form 28 June 2021; Accepted 29 July 2021
Available online 2 August 2021

**Abbreviations**

| | |
|---|---|
| ANOVA | Analysis of variance |
| ANXA2 | Annexin A2 |
| CGRP | Calcitonin gene-related peptide |
| co-IP | Co-immunoprecipitation |
| DAMGO | [D-Ala$^2$-MePhe$^4$-Gly$^5$-ol] enkephalin |
| DAPI | 4′,6-diamidino-2-phenylindole |
| dd$H_2O$ | Double-distilled water |
| DMEM | Dulbecco's modified eagle's medium |
| DRG | dorsal root ganglion |
| FBS | foetal bovine serum |
| FKBP12 | FK506 binding protein 12 |
| GPCRs | G-protein-coupled receptors |
| HEK293 | Human embryonic kidney 293 |
| HPLC-MS/MS | High performance liquid chromatography with tandem mass spectrometry |
| IB4 | Isolectin B4 |
| IP | Immunoprecipitation |
| LASEC | Laboratory Animal Services Centre |
| LPS | lipopolysaccharide |
| MIPs | MOR-interacting proteins |
| MOR | Mu-opioid receptors |
| PBS | Phosphate-buffered saline |
| PVDF | polyvinylidene difluoride |
| RIPA | Radioimmunoprecipitation assay |
| SDS | Sodium dodecyl sulfate |
| SEM | standard error of mean |
| TLR4 | Toll-like Receptor 4 |

identification and functional characterization of novel MOR-interacting proteins will help to delineate cellular and molecular mechanism of action of remifentanil. In this study, we identified novel MOR-interacting proteins (MIPs) using formaldehyde cross-linking and immunoprecipitation. The roles of MIPs on MOR sorting and subcellular location were then investigated. Our findings may aid understanding the molecular mechanisms underlying remifentanil-induced receptor redistribution.

## *Materials and methods*

### *Cell cultures*

All reagents were purchased from Life Technologies, Carlsbad, CA, USA, unless otherwise specified. Human embryonic kidney 293 (HEK293) cells (ATCC, Manassas, VA, USA) were cultured in Dulbecco's modified eagle's medium (DMEM) supplemented with 10% foetal bovine serum (FBS) and 1% antibiotic–antimycotic. All cells were cultured at 37 °C with 5% carbon dioxide in humidified atmosphere. Remifentanil hydrochloride (Ultiva, Abbott, Chicago, IL, USA) was used in this study.

### *Animals*

250–300 g male Sprague Dawley rats were used in this study. All rats were provided by the Laboratory Animal Services Centre (LASEC), the Chinese University of Hong Kong. The animals were housed in groups per cage with animal chow and water ad libitum on a 12 h light/dark cycle at 23 ± 2 °C. All animal experimental procedures were approved by the Animal Experimentation Ethics Committee of the Chinese University of Hong Kong.

### *Plasmid construction and cell transfection*

Human *MOR* and *ANXA2* genes from U-251 cells-derived cDNA were cloned into pcDNA3.1-mCherry and pcDNA3.1-EGFP backbone plasmids, respectively. Primer sequences for pMOR-mCherry are: sense, 5′-CGAGCTCAAGCTTCGATGGACAGCAGCGCTGC-3′; antisense, 5′-GGCGACCGGTGGATCGGGCAACGGAGCAGTTTC-3′. Primer sequences for pANXA2-EGFP are: sense, 5′-TCCGGACTCAGATCTATGGGCCGCCAGCTAGC-3′; antisense, 5′-GTCGACTGCAGAATTCTAGTCATCTCCACCACACAG-3′. Cell transfection was performed using Lipofectamine 2000: plasmid (2:1) mixtures according to the manufacturer's instructions.

### *Formaldehyde cross-linking and immunoprecipitation (IP), silver staining and high-performance liquid chromatography with tandem mass spectrometry (HPLC-MS/MS)*

U-251 MG cells were re-suspended to 1 × $10^7$ cells/ml, exposed to and pelleted in formaldehyde solution or phosphate-buffered saline (PBS) for 10 min before quenching with ice-cold 1.25 M glycine/PBS. Cells were then lysed in 1 ml radioimmunoprecipitation assay (RIPA) buffer (50 mM Tris HCl, pH 8.0, 150 mM sodium chloride, 1% NP-40, 0.5% sodium deoxycholate), 1 mM EDTA, protease inhibitors (Complete mini, EDTA-free, Roche Diagnostics, Basel, Switzerland) per 1 × $10^8$ cells for 60 min on ice. Cell lysates were pre-cleared with protein G magnetic beads for 2 h then incubated with antibodies and beads overnight with gentle agitation at 4 °C. The beads were washed three times with RIPA buffer and denatured in 4 × reducing SDS Loading dye [500 mM Tris HCl, pH 6.8, 8% sodium dodecyl sulfate (SDS), 40% glycerine, 20% β-mercaptoethanol, 5 mg/ml bromophenol blue] for SDS/PAGE analysis. Silver staining was carried out using Pierce Silver staining kit (ThermoFisher Scientific, Waltham, MA, USA) according to manufacturers' protocol. Briefly, gels were fixed in 10% (v/v) acetic acid/30% (v/v) ethanol for 15 min, rinsed with double-distilled water (dd$H_2O$) for 10 min twice and sensitized with sensitizer working solution for 1 min. The gels were then rinsed three times in dd$H_2O$ before 10-minute incubation in stain working solution. Acetic acid was used to quench the developing reaction. Specific bands compared to IgG-IP were excised and sent for HPLC-MS/MS (N-Cell Technology, Ltd. Shenzhen, China).

### *Co-immunoprecipitation*

Rat DRG tissue was freshly harvested and immediately lysed in lysis buffer. Co-immunoprecipitation (co-IP) was performed using protein G magnetic beads as described above according to manufacturer's protocol. Cell lysates were incubated with antibodies and beads overnight with gentle agitation at 4 °C. The beads were then rinsed twice with PBS and denatured in 4 × reducing SDS Loading dye for SDS/PAGE analysis. Antibodies against ANXA2 (Santa Cruz Biotechnology, Santa Cruz, CA) were used for co-IP.

### *Western blots*

Denatured cell lysate in loading dye was subjected to SDS/PAGE in 10% or 15% gels. Separated proteins were transferred to polyvinylidene difluoride (PVDF) membrane (Millipore, Billerica, MA, USA), blocked with 5% (w/v) skim milk for 1 h and incubated with primary antibodies against MOR, ANXA2 or β-actin (Santa Cruz Biotechnology, Santa Cruz, CA) overnight at 4 °C. The membranes were rinsed and incubated with horseradish peroxidase-conjugated anti-mouse or rabbit secondary antibodies (Cell signalling technology, Beverly, MA, USA) for 1 h at room temperature. Enhanced chemiluminescence detection system (GE Healthcare Biosciences, Pittsburgh, PA, USA) was used for band visualization.

### *Immunohistochemistry*

Rat DRG tissue was fixed in 4% paraformaldehyde followed by 30%

sucrose solution cryopreservation and cryosectioning. Transfected HEK293T cells were plated onto cover slips, treated and fixed in 4% (w/v) paraformaldehyde. Standard immunohistochemistry protocol was performed using antibodies against ANXA2 (Santa Cruz Biotechnology, Santa Cruz, CA, USA), OPRM1 (R&D Systems, Minneapolis, MN, USA), mCherry (ImmunoWay Biotechnology Company, Plano, TX, USA), Rab11 (Abcam, Cambridge, UK), CGRP (Sigma-Aldrich, St. Louis, MO, USA), Substance P (Sigma-Aldrich, St. Louis, MO, USA) and Isolectin GS-IB4 (ThermoFisher Scientific, Waltham, MA, USA). Samples were mounted with ProLong Gold Antifade Mountant with 4′,6-diamidino-2-phenylindole (DAPI) (ThermoFisher Scientific, Waltham, MA, USA) for examination using confocal microscopy.

*Single-cell RNA-seq analysis*

DRG neuron single-cell RNA sequencing (scRNA-seq) dataset (GSE63576) was publicly available. Data extraction and graph preparation were performed with R (version 4.0.3). Marker genes for DRG neuronal cluster 1–10 were reported (Li et al., 2016).

*Statistical analysis*

The degree of co-localization of the fluorescence signal was determined using an in-built image analysis software of SP8 TCS confocal microscopy platform (Leica, Wetzlar, Germany) and represented as relative Pearson's correlation index. Membrane MOR intensity analysis was performed with ImageJ. Data were expressed as the mean ± standard error of mean (SEM). Analysis of variance (ANOVA) was used and followed by post-hoc Tukey's or Bonferroni tests for correction of multiple comparisons. Spearman's correlation analysis was performed for Oprm1 and Anxa2 using the scRNA-seq dataset.

*Results*

*Identification of ANXA2 as a novel MOR-interacting protein*

MOR-interacting proteins play important roles in modulating MOR1 signalling. We first conducted formaldehyde cross-linking and IP to isolate MOR signalling complexes from U-251 MG glioblastoma cells (Fig. 1**A**). Silver staining of the SDS-PAGE showed that there were multiple specific bands in the cross-linking IP lanes, compared to anti-IgG negative control (Fig. 1**B**). These specific bands were sent for protein identification using HPLC-MS/MS. Ninety-six candidate proteins were identified, two of which (GTPase and mGluR5) are previously identified MOR-interacting proteins (**Supplementary Table 1**). Of note, ANXA2 had the highest ion score (**Supplementary Table 1**) and peptide number (Fig. 1**C, 2B, C and Supplementary Figure S1**). ANXA2 was therefore chosen as the potential novel MOR-interacting protein candidate for further study.

*ANXA2 was a MOR-interacting protein in rat DRG*

To confirm that ANXA2 was an *in vivo* MOR-interacting protein, we performed staining and co-IP using rat DRG tissue. Immunofluorescence

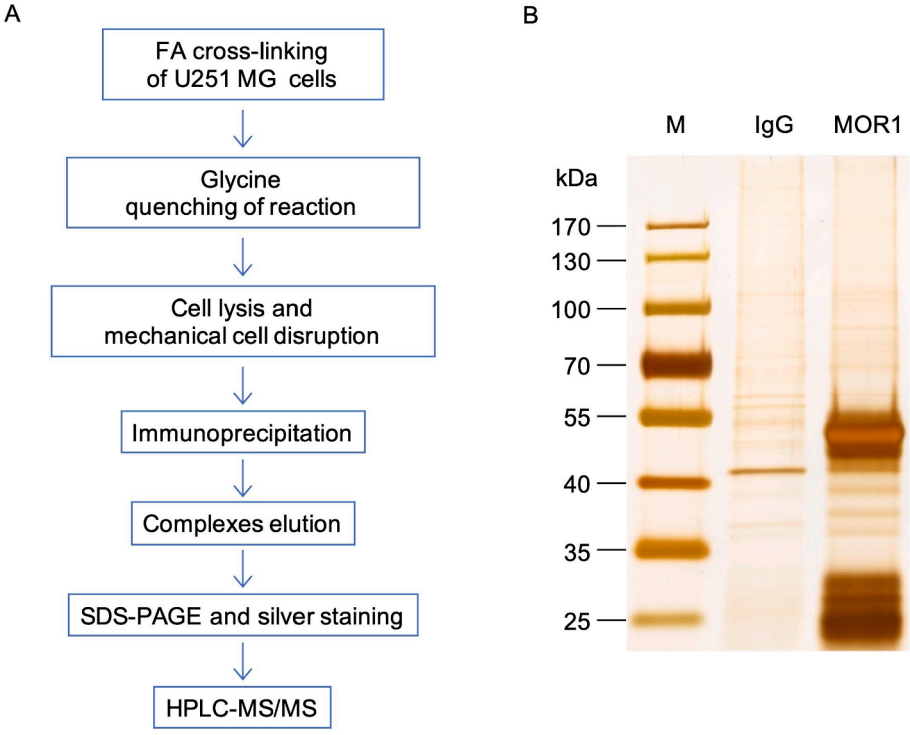


**Fig. 1.** Identification of ANXA2 as a novel MOR1-interacting protein. (A) A flow diagram showing the procedures of formaldehyde (FA) cross-linking immunoprecipitation for MOR-interacting protein identification. (B) Silver staining of MOR-interacting proteins separated in SDS-PAGE. M, Marker; IgG, antibodies against rabbit IgG as negative control; MOR1, antibodies against MOR1. (C). Peptide fragments, highlighted in bold letters, identified by HPLC/MS-MS in human ANXA2 amino acid sequence.

C

MGRQLAGCGDAGKKASFKMSTVHEILCKLSLEGDHSTPPSAYGSVKAYTNFDAERDALNIETAIKTKGVD

EVTIVNILTNRSNAQRQDIAFAYQRRTKKELASALKSALSGHLETVILGLLK**TPAQYDASELK**ASMKGLG

TDEDSLIEIICSR**TNQELQEINR**VYKEMYKTDLEKDIISDTSGDFRKLMVALAKGRRAEDGSVIDYELID

QDARDLYDAGVKRKGTDVPK**WISIMTER**SVPHLQKVFDRYKSYSPYDMLESIRKEVKGDLENAFLNLVQC

IQNKPLYFADRLYDSMKGKGTRDKVLIRIMVSRSEVDMLKIRSEFKRKYGKSLYYYIQQDTKGDYQKALL

YLCGGDD

assay was performed to determine the distribution of ANXA2 and MOR1 in rat DRG tissues. Confocal microscopy confirmed that ANXA2 and MOR1 were co-localized in cytoplasm and on cell membrane (Fig. 2**A**). Additional immunofluorescence assays showed that ANXA2 and MOR1 were co-localized in DRG neuronal populations. Specifically, the two proteins were expressed in peptidergic subsets expressing neuropeptide substance P and calcitonin gene-related peptide (CGRP, **Supplementary figure S2A and B**), and peptidergic subset expressing isolectin B4 (IB4, **(Supplementary figure S2C)** (Ju et al., 1987; Nagy and Hunt, 1982; Silverman and Kruger, 1990). We also evaluated the differential expression of Oprm1 and Anxa2 in a publicly available DRG neuron scRNA-seq dataset (GSE63576). Both Oprm1 and Anxa2 were identified in a subset of neuronal population **(Supplementary figure S2D)** (Li et al., 2016). Correlation analysis indicated a positive association between Oprm1 and Anxa2 (rho = 0.39, $p = 6.9 \times 10^{-9}$, **Supplementary figure S2E**). Oprm1 and Anxa1 selectively co-expressed in neurons expressing markers (high level of Nppb, Il31ra, Nts and Htr1f) of neuronal cluster 2 (C2, **Supplementary figure S2F**), which was reported to respond to heat and pinch but not pressure (Li et al., 2016). Collectively, these results suggested that MOR1 and ANXA2 were co-expressed in DRG neurons. Following the spatial overlap of ANXA2 and MOR1 in DRG neurons, co-IP using rat DRG tissues was performed to demonstrate the interaction between the two proteins. Western blots showed that MOR1 was immunoprecipitated by anti-ANXA2 antibodies. No MOR1 was detected when rabbit IgG antibodies were used for mock co-IP (Fig. 2**B**).

*Reduced MOR1 redistribution to plasma membrane after internalization by enforced expression of ANXA2*

Less accessible opioid receptors on the cell membrane was considered as a potential mechanism for acute opioid tolerance caused by remifentanil (Nowoczyn et al., 2013). Consistent with previous studies, our cellular assay showed that 3 h of remifentanil treatment induced reduction of membrane mCherry-tagged MOR1 immunofluorescence in a dose-dependent manner (Fig. 3**A and B**). This slowly recovered in a period lasting more than 3 h after drug washout (Fig. 3**C**). To explore the role of ANXA2 in MOR1 internalization, we overexpressed eGFP-tagged ANXA2 in HEK293 cells transfected with MOR1-mCherry. As demonstrated in Fig. 3B and C, ANXA2 overexpression further significantly reduced cell surface availability of MOR1 and slowed down the redistribution of MOR to the cell membrane.

*Trapping of MOR1 in late endosomes by ANAX2*

In general, MOR1 internalization was followed by rapid (within 1 h) plasma membrane re-distribution that was carried by recycling endosomes. However, remifentanil caused unexpectedly long MOR1 recycling time (greater than 3 h). We tested if remifentanil could "mislead" the sorting of MOR1 to alternative intracellular structures. We performed immunofluorescence staining to visualize recycling endosome marker Rab11 in HEK293 cells transfected with MOR1-mCherry and

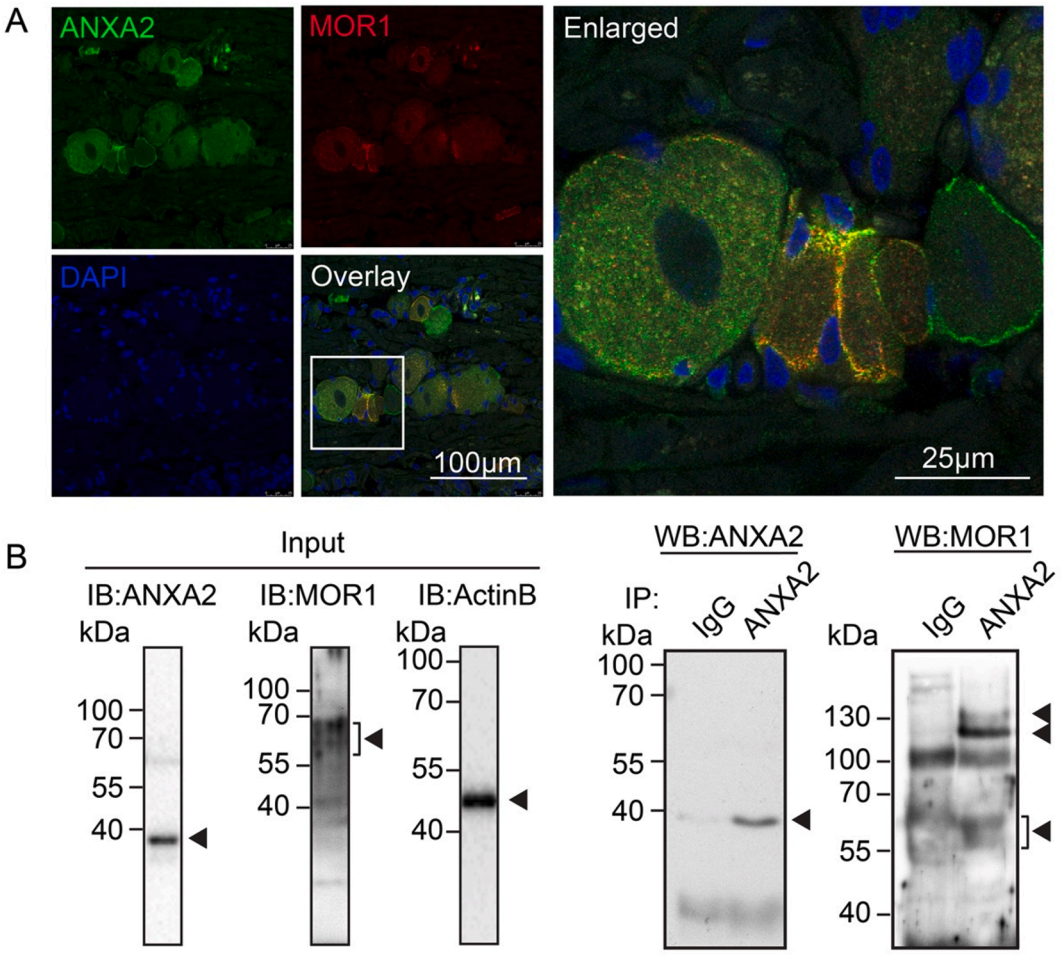


**Fig. 2.** MOR1 interacted with ANXA2 in rat dorsal root ganglion tissue. (A) Immunofluorescence assay of ANXA2 and MOR1 in rat dorsal root ganglion tissue. Green, ANXA2. Red, MOR1. Blue, DAPI. (B) Immunoblots of co-immunoprecipitated proteins from rat dorsal root ganglion tissue using anti-ANXA2 antibodies. IP, immunoprecipitation; WB, western blotting; MOR1, anti-MOR1 antibodies; ANXA2, anti-ANXA2 antibodies; b-actin, anti-β-actin antibodies; IgG, anti-rabbit IgG antibodies. Arrows indicate specific bands in each blot.

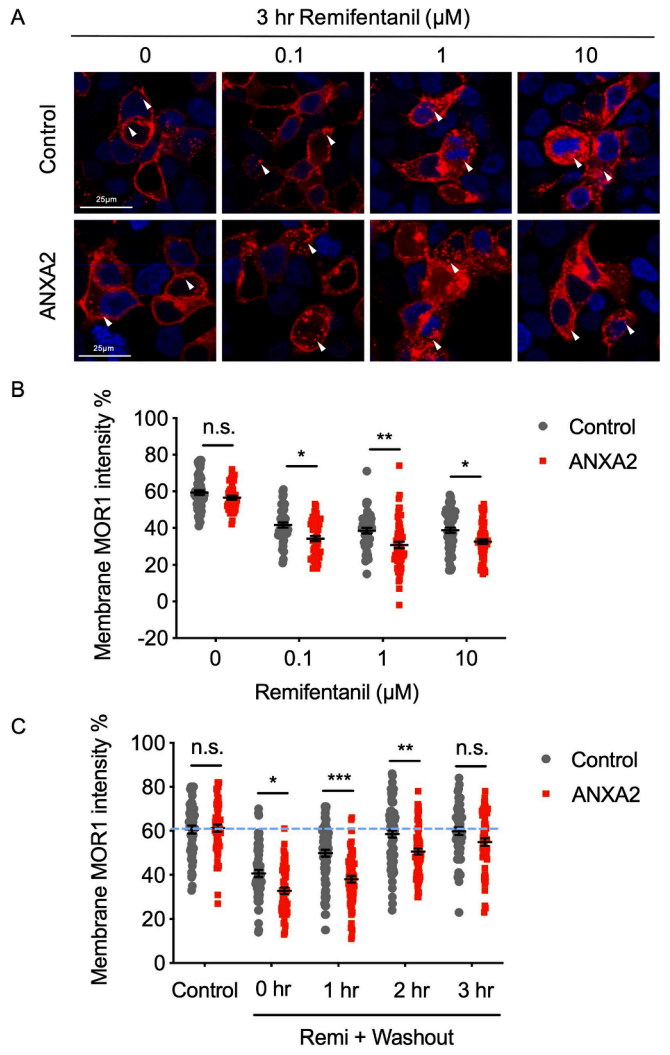


**Fig. 3.** ANXA2 overexpression delayed the membrane MOR1 re-distribution after remifentanil washout. (A) Remifentanil reduced mCherry-tagged MOR1 cell membrane immunofluorescence intensities in a dose-dependent fashion. HEK293 cells with mCherry-MOR1 overexpression were treated with various doses of remifentanil for 3 hours. Enforced expression of ANXA2 further reduced MOR1 cell membrane distribution. Arrowheads, internalized MOR1 vesicles. (B) Immunofluorescence intensities quantification of A ($n = 41$ to 60 cells each group from 5 independent experiments. $p < 0.001$, factorial ANOVA). (C) Immunofluorescence intensities of mCherry-tagged MOR1 recycled to plasma membrane after remifentanil washout (for 3 hours) was delayed by ANXA2 overexpression ($n = 48$ to 78 cells for each group from 5 independent experiments. $p < 0.001$ factorial ANOVA). n.s., non-significant, *, $p < 0.05$ and **, $p < 0.01$ compared to control group with Tukey's multiple comparison tests.

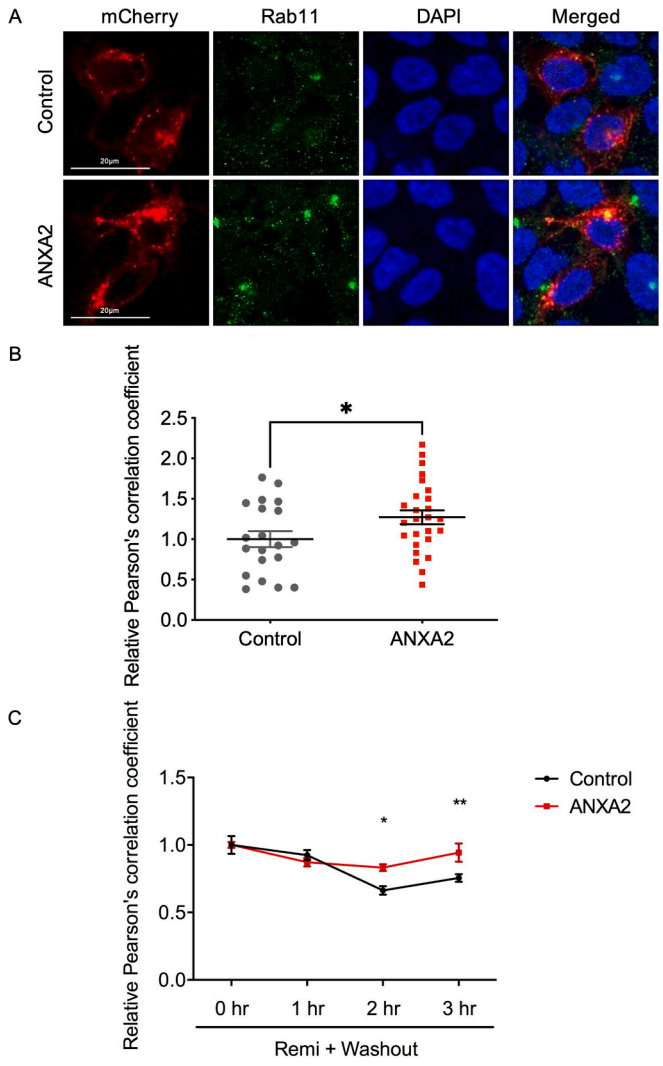


**Fig. 4.** ANXA2 contributed to the retention of MOR1 in the cytoplasmic compartment. (A) Remifentanil induced MOR1 co-localization to the late recycling endosome marker Rab11. (B) Quantification of co-localization of MOR1 and Rab11. Relative Pearson's correlation indicated MOR1 and Rab11 co-localization. In comparison with the control plasmid, ANXA2 overexpression increased colocalization of MOR with Rab11. $n = 20$ for Control, $n = 26$ for ANXA2 overexpression. *, $p < 0.05$, Student's $t$ test. (C) ANXA2 overexpression delayed MOR1 recycling after remifentanil washout ($p < 0.001$, factorial ANOVA). Remi, Remifentanil. $n = 40$ cells each group from 3 independent experiments. *, $p < 0.05$ and **, $p < 0.01$, adjusted by Bonferroni correction.

ANXA2 (**Supplementary Figure S3**). Surprisingly, we found that remifentanil caused high level of co-localization of MOR1 and Rab11, indicative of re-distribution of MOR1 in recycling endosomes. Of note, ANXA2 overexpression further increased the co-localization of MOR1 and Rab11 (Fig. 4**A and B**). When remifentanil was washed out, the co-localization of MOR1 and Rab11 was reduced in a time-dependent fashion, as indicated by the Pearson's correlation coefficient. However, in the presence of ANXA2 overexpression, the coefficient remained stable from 0 to 3 h (Fig. 4**C**). This suggested that ANXA2 retarded MOR1 recycling after remifentanil washout by trapping MOR1 in "slow" recycling endosomes (Naslavsky and Caplan, 2018).

## *Discussion*

Intraoperative infusion of high-dose remifentanil (cumulative dose of ≥ 25 μg/kg) has been repeatedly reported to cause higher post-operative opioid requirement, indicative of an acute opioid tolerance. The underlying mechanisms remain elusive. In this study, we identified ANXA2 as a novel MOR1-interacting protein that retards membrane re-localization of MOR1 after remifentanil treatment. We showed that in the presence of remifentanil, ANXA2 overexpression sorted MOR1 to late endosomes, which in turn retarded cell surface distribution of MOR1 after remifentanil withdrawal. Our study therefore provided a plausible mechanism, where ANXA2-mediated reduction of MOR1 availability in the cell membrane.

The molecular network driving opioid tolerance development varies among different types of opioids or treatment paradigms. With respect to the types of opioids, agonist-selective MOR1 internalization has been considered as an important mechanism to prevent acute opioid

tolerance development. For instance, [D-Ala$^2$-MePhe$^4$-Gly$^5$-ol] enkephalin (DAMGO) rapidly induces MOR1 endocytosis within 30 min after treatment. Consistent with this, repeated administration of DAMGO did not induce acute opioid tolerance. Knockdown of dynamin abolished DAMGO-induced MOR1 internalization and caused DAMGO tolerance (Ueda et al., 2001). In contrast, opioid-induced acute analgesic tolerance could be prevented by PKC inhibition (Ueda et al., 2001) or knockdown of cellular FK506 binding protein 12 (FKBP12) (Yan et al., 2014), which leads to MOR1 internalization. One plausible theory underlying these processes is that MOR1 internalization followed by rapid recycling contributes to its functional re-sensitization and counteracts opioid tolerance (Koch and Höllt, 2008). However, MOR1 internalization without rapid recycling would lead to reduced MOR1 cell surface availability and contribute to opioid tolerance. In this regard, chronic opioid treatment has been revealed to cause persistent MOR1 internalization in neurons along with the establishment of opioid tolerance (Drake et al., 2005). Opioid-induced MOR1 internalization was frequently observed in the nervous system. Morphine pellets, which constantly release this opioid after implantation, caused significant MOR internalization in the spinal cord from 3 h to 48 h. However, morphine analgesia declined from 2 h and disappeared after 12 h, indicating that prolonged receptor internalization could not prevent opioid tolerance (Rodriguez-Munoz et al., 2007). For remifentanil, short-term administration (1 h) induced elevation of intracellular MOR1-mCherry puncta numbers but reduction of mCherry plasma membrane fluorescence, implying that remifentanil caused MOR1 internalization. It should be noted that, after remifentanil washout, reduced MOR1 membrane expression sustained for at least 3 h, compared with the vehicle group. Prolonged MOR1 internalization following remifentanil administration thus may not refer to receptor re-sensitization. Instead, it may cause deficient responses of other MOR1 agonists (e.g. morphine) to the cells. Our study highlighted that a time-dependent subcellular redistribution of MOR1 after remifentanil administration should be explored in future animal studies to delineate the mechanisms of remifentanil-related MOR receptor redistribution. Meanwhile, we found that enforced expression of ANXA2 further delayed the recovery of cell membrane distribution of MOR1, inferring that ANXA2 may play a role in this process. In contrast, ANXA2 overexpression did not affect DAMGO-induced MOR1 cell membrane internalization (**Supplementary Figure S4**), indicating the function of ANXA2 on MOR1 recycling is agonist-specific. More noteworthy is that opioid tolerance is a complex process that involves the interplay of individual cellular responses, as well as recruitment of different neuronal circuits, suggesting that receptor trafficking alone is insufficient to produce morphine tolerance (Williams et al., 2013). The contribution of ANXA2-induced MOR1 recycling to analgesic tolerance requires further investigation.

ANXA2 has been shown to promote internalization of several membrane proteins. For instance, ANXA2 is critical for Toll-Like Receptor 4 (TLR4) internalization in response to lipopolysaccharide (LPS) binding. In keeping with this, ANXA2 knockout leads to sustained TLR4 membrane expression and aggravated inflammatory response (Zhang et al., 2015). In this study, we identified ANXA2 as a novel MOR1-interacting protein. Moreover, ANXA2 facilitated MOR1 internalization after remifentanil administration, indicative of a similar action of ANXA2 on TLR4. Our studies suggested that ANXA2-mediated actions represent a common mechanism for receptor internalization. Indeed, intracellular TLR4 was sorted mainly to early-endosomes by ANXA2, which is also evident as for MOR1. In addition, we observed that MOR1 was co-localized with Rab11 (a marker of recycling endosomes) after remifentanil treatment. However, remifentanil-induced binding to recycling endosomes did not lead to rapid MOR1 redistribution on the cell surface. Instead, MOR1 was “trapped” in the endosomes for at least 3 h after remifentanil exposure. It is possible that deferred membrane redistribution of MOR1 might contribute to opioid receptor tolerance, in which a subsequently higher dose of morphine is required to achieve sufficient analgesia, resulting in morphine tolerance.

## Conclusions

Taken together, we reported that ANXA2 retarded membrane redistribution of MOR1 after remifentanil exposure. Interventions targeting ANXA2 might represent a novel approach to maintain adequate cell-surface MOR and thus morphine analgesia after remifentanil administration.

## Funding

This work was supported by the Anesthesia and Pain Medicine Foundation, Australian and New Zealand College of Anaesthetists [grant number #17-013].

## CRediT authorship contribution statement

**Idy H.T. Ho:** Investigation, Visualization, Writing - original draft. **Lhotse H.L. Ng:** Validation. **Xiaojie Cheng:** Conceptualization. **Tony Gin:** Writing - review & editing. **Chee Sam Chan:** Validation. **Wuping Sun:** Writing - review & editing. **Lizu Xiao:** Writing - review & editing. **Lin Zhang:** Writing - review & editing. **Matthew T.V. Chan:** Funding acquisition, Supervision, Writing - review & editing. **William K.K. Wu:** Supervision, Writing - review & editing. **Xiaodong Liu:** Investigation, Project administration, Writing - original draft.

## Declaration of Competing Interest

The authors declare that there is no conflict of interest regarding the publication of this paper.

## Appendix A. Supplementary data

Supplementary data to this article can be found online at https://doi.org/10.1016/j.ynpai.2021.100071.

## References

Thompson, J.P., Rowbotham, D.J., 1996. Remifentanil–an opioid for the 21st century. Br J Anaesth 76 (3), 341–343. https://doi.org/10.1093/bja/76.3.341.

Komatsu, R., Turan, A.M., Orhan-Sungur, M., McGuire, J., Radke, O.C., Apfel, C.C., 2007. Remifentanil for general anaesthesia: a systematic review. Anaesthesia 62, 1266–1280. https://doi.org/10.1111/j.1365-2044.2007.05221.x.

Guignard, B., Bossard, A.E., Coste, C., Sessler, D.I., Lebrault, C., Alfonsi, P., Fletcher, D., Chauvin, M., 2000. Acute opioid tolerance: intraoperative remifentanil increases postoperative pain and morphine requirement. Anesthesiology 93, 409–417. https://doi.org/10.1097/00000542-200008000-00019.

Crawford, M.W., Hickey, C., Zaarour, C., Howard, A., Naser, B., 2006. Development of acute opioid tolerance during infusion of remifentanil for pediatric scoliosis surgery. Anesth Analg 102 (6), 1662–1667. https://doi.org/10.1213/01.ane.0000216036.95705.c2.

Suhitharan, T., Subramani, S., Win, M.T.M., Sulaiman, W.B., Johar, N.B., Chi, O.B., 2018. Effect of remifentanil on the recovery profile after head and neck surgeries: a prospective study. J. Anaesthesiol. Clin. Pharmacol. 34, 307–313. https://doi.org/10.4103/joacp.JOACP_337_16.

Wu, J.X., Assel, M., Vickers, A., Afonso, A.M., Twersky, R.S., Simon, B.A., Cohen, M.A., Rieth, E.F., Cracchiolo, J.R., 2019. Impact of intraoperative remifentanil on postoperative pain and opioid use in thyroid surgery. J. Surg. Oncol. 120 (8), 1456–1461. https://doi.org/10.1002/jso.v120.810.1002/jso.25746.

de Hoogd, S., Ahlers, S.J.G.M., van Dongen, E.P.A., van de Garde, E.M.W., Daeter, E.J., Dahan, A., Tibboel, D., Knibbe, C.A.J., 2018. Randomized controlled trial on the influence of intraoperative remifentanil versus fentanyl on acute and chronic pain after cardiac surgery. Pain Pract. 18 (4), 443–451. https://doi.org/10.1111/papr.2018.18.issue-410.1111/papr.12615.

Sanfilippo, F., Conticello, C., Santonocito, C., Minardi, C., Palermo, F., Bernardini, R., Gullo, A., Astuto, M., 2016. Remifentanil and worse patient-reported outcomes regarding postoperative pain management after thyroidectomy. J. Clin. Anesth. 31, 27–33. https://doi.org/10.1016/j.jclinane.2015.12.025.

Grape, S., Kirkham, K.R., Frauenknecht, J., Albrecht, E., 2019. Intra-operative analgesia with remifentanil vs. dexmedetomidine: a systematic review and meta-analysis with trial sequential analysis. Anaesthesia 74, 793–800. https://doi.org/10.1111/anae.14657.

Fletcher, D., Martinez, V., 2014. Opioid-induced hyperalgesia in patients after surgery: a systematic review and a meta-analysis. Br. J. Anaesth. 112, 991–1004. https://doi.org/10.1093/bja/aeu137.

Motamed, C., Audibert, J., Albi-Feldzer, A., Bouroche, G., Jayr, C., 2017. Postoperative pain scores and opioid consumption in opioid-dependent patients with cancer after intraoperative remifentanil analgesia: A prospective case-controlled study. J. Opioid Manag. 13, 221–228. https://doi.org/10.5055/jom.2017.0390.

Vinik, H.R., Kissin, I., 1998. Rapid development of tolerance to analgesia during remifentanil infusion in humans. Anesth. Analg. 86, 1307–1311. https://doi.org/10.1097/00000539-199806000-00033.

Wang, D., Tawfik, V.L., Corder, G., Low, S.A., François, A., Basbaum, A.I., Scherrer, G., 2018. Functional divergence of delta and mu opioid receptor organization in CNS pain circuits. Neuron 98 (1), 90–108.e5. https://doi.org/10.1016/j.neuron.2018.03.002.

Williams, J.T., Ingram, S.L., Henderson, G., Chavkin, C., von Zastrow, M., Schulz, S., Koch, T., Evans, C.J., Christie, M.J., 2013. Regulation of mu-opioid receptors: desensitization, phosphorylation, internalization, and tolerance. Pharmacol. Rev. 65, 223–254. https://doi.org/10.1124/pr.112.005942.

Georgoussi, Z., Georganta, E.M., Milligan, G., 2012. The other side of opioid receptor signalling: regulation by protein-protein interaction. Curr. Drug Targets 13, 80–102. https://doi.org/10.2174/138945012798868470.

Milligan, G., 2005. Opioid receptors and their interacting proteins. Neuromol. Med. 7 (1-2), 051–060. https://doi.org/10.1385/NMM:7:1-210.1385/NMM:7:1-2:051.

Petko, J., Justice-Bitner, S., Jin, J., Wong, V., Kittanakom, S., Ferraro, T.N., Stagljar, I., Levenson, R., 2013. MOR is not enough: identification of novel mu-opioid receptor interacting proteins using traditional and modified membrane yeast two-hybrid screens. PLoS One 8, e67608. https://doi.org/10.1371/journal.pone.0067608.

Marie, N., Aguila, B., Allouche, S., 2006. Tracking the opioid receptors on the way of desensitization. Cell Signal 18 (11), 1815–1833. https://doi.org/10.1016/j.cellsig.2006.03.015.

Jaremko, K.M., Thompson Jr., N.L., Reyes, B.A., Jin, J., Ebersole, B., Jenney, C.B., Grigson, P.S., Levenson, R., Berrettini, W.H., Van Bockstaele, E.J., 2014. Morphine-induced trafficking of a mu-opioid receptor interacting protein in rat locus coeruleus neurons. Prog. Neuropsychopharmacol. Biol. Psychiatry 50, 53–65. https://doi.org/10.1016/j.pnpbp.2013.12.003.

Charlton, J.J., Allen, P.B., Psifogeorgou, K., Chakravarty, S., Gomes, I., Neve, R.L., Devi, L.A., Greengard, P., Nestler, E.J., Zachariou, V., 2008. Multiple actions of spinophilin regulate mu opioid receptor function. Neuron 58 (2), 238–247. https://doi.org/10.1016/j.neuron.2008.02.006.

Li, C.-L., Li, K.-C., Wu, D., Chen, Y., Luo, H., Zhao, J.-R., Wang, S.-S., Sun, M.-M., Lu, Y.-J., Zhong, Y.-Q., Hu, X.-Y., Hou, R., Zhou, B.-B., Bao, L., Xiao, H.-S., Zhang, X., 2016. Somatosensory neuron types identified by high-coverage single-cell RNA-sequencing and functional heterogeneity. Cell Res 26 (1), 83–102. https://doi.org/10.1038/cr.2015.149.

Ju, G., Hokfelt, T., Brodin, E., Fahrenkrug, J., Fischer, J.A., Frey, P., Elde, R.P., Brown, J.C., 1987. Primary sensory neurons of the rat showing calcitonin gene-related peptide immunoreactivity and their relation to substance P-, somatostatin-, galanin-, vasoactive intestinal polypeptide- and cholecystokinin-immunoreactive ganglion cells. Cell Tissue Res 247, 417–431. https://doi.org/10.1007/BF00218323.

Nagy, J.I., Hunt, S.P., 1982. Fluoride-resistant acid phosphatase-containing neurones in dorsal root ganglia are separate from those containing substance P or somatostatin. Neuroscience 7 (1), 89–97. https://doi.org/10.1016/0306-4522(82)90155-5.

Silverman, J.D., Kruger, L., 1990. Selective neuronal glycoconjugate expression in sensory and autonomic ganglia: relation of lectin reactivity to peptide and enzyme markers. J. Neurocytol. 19, 789–801. https://doi.org/10.1007/BF01188046.

Nowoczyn, M., Marie, N., Coulbault, L., Hervault, M., Davis, A., Hanouz, J.L., Allouche, S., 2013. Remifentanil produces cross-desensitization and tolerance with morphine on the mu-opioid receptor. Neuropharmacology 73, 368–379. https://doi.org/10.1016/j.neuropharm.2013.06.010.

Naslavsky, N., Caplan, S., 2018. The enigmatic endosome - sorting the ins and outs of endocytic trafficking. J. Cell Sci. 131 https://doi.org/10.1242/jcs.216499.

Ueda, H., Inoue, M., Matsumoto, T., 2001. Protein kinase C-mediated inhibition of mu-opioid receptor internalization and its involvement in the development of acute tolerance to peripheral mu-agonist analgesia. J. Neurosci. 21, 2967–2973.

Yan, Y.H., Wang, Y., Zhao, L.X., Jiang, S., Loh, H.H., Law, P.Y., Chen, H.Z., Qiu, Y., 2014. Role of FK506 binding protein 12 in morphine-induced mu-opioid receptor internalization and desensitization. Neurosci. Lett. 566, 231–235. https://doi.org/10.1016/j.neulet.2014.02.059.

Koch, T., Höllt, V., 2008. Role of receptor internalization in opioid tolerance and dependence. Pharmacol. Ther. 117 (2), 199–206. https://doi.org/10.1016/j.pharmthera.2007.10.003.

Drake, C.T., Aicher, S.A., Montalmant, F.L., Milner, T.A., 2005. Redistribution of mu-opioid receptors in C1 adrenergic neurons following chronic administration of morphine. Exp. Neurol. 196 (2), 365–372. https://doi.org/10.1016/j.expneurol.2005.08.012.

Rodriguez-Munoz, M., de la Torre-Madrid, E., Sanchez-Blazquez, P., Garzon, J., 2007. Morphine induces endocytosis of neuronal mu-opioid receptors through the sustained transfer of Galpha subunits to RGSZ2 proteins. Mol. Pain 3, 19. https://doi.org/10.1186/1744-8069-3-19.

Zhang, S., Yu, M., Guo, Q., Li, R., Li, G., Tan, S., Li, X., Wei, Y., Wu, M., 2015. Annexin A2 binds to endosomes and negatively regulates TLR4-triggered inflammatory responses via the TRAM-TRIF pathway. Sci. Rep. 5, 15859. https://doi.org/10.1038/srep15859.